Journal of Catalysis 256 (2008) 183–191

Contents lists available at ScienceDirect

Journal of Catalysis

www.elsevier.com/locate/jcat

The catalytic performance of Cu-containing zeolites in N_2O decomposition and the influence of O_2, NO and H_2O on recombination of oxygen

Pieter J. Smeets [a], Bert F. Sels [a], Robert M. van Teeffelen [b], Hugo Leeman [a], Emiel J.M. Hensen [b], Robert A. Schoonheydt [a,*]

[a] Center for Surface Chemistry and Catalysis, K.U. Leuven, Kasteelpark Arenberg 23, B-3001 Leuven, Belgium
[b] Schuit Institute of Catalysis, Eindhoven University of Technology, P.O. Box 513, 5600 MB Eindhoven, The Netherlands

ARTICLE INFO

Article history:
Received 30 November 2007
Revised 19 February 2008
Accepted 14 March 2008
Available online 24 April 2008

Keywords:
N_2O decomposition
NO
Water
Cu-zeolites
Mechanism
Kinetics

ABSTRACT

The catalytic decomposition of N_2O was studied over Cu-containing zeolites with different Cu loadings and framework topologies (MFI, MOR, FER, BEA, and FAU). The influence of NO, O_2, and H_2O on the rate of N_2O decomposition was investigated in detail. A kinetic model was developed based on the relevant elementary reaction steps in the mechanism of N_2O decomposition. The recombination of oxygen atoms into molecular oxygen is recognized as the rate-limiting step in N_2O decomposition. The rate of oxygen desorption depends strongly on the Cu loading. At low Cu loadings, migration of oxygen atoms is required for recombinative desorption. NO accelerates oxygen recombination, because it provides an alternative route for oxygen migration via gas-phase NO_2. The effect of water differs for Cu-containing zeolites with high and low Cu loadings. At high Cu loading, the rate is suppressed by competitive adsorption of water on the active sites, resulting in an increase in apparent activation energy. The rate of N_2O decomposition is increased substantially for catalysts with a low Cu loading. This is tentatively attributed to water-induced mobility of Cu ions, which facilitates oxygen migration. The effect of water addition is fully reversible.

1. Introduction

Cu-containing zeolites have been widely investigated in direct NO and N_2O decomposition [1–16] as well as in the selective catalytic reduction (SCR) of NO_x and N_2O by light hydrocarbons [17,18], NH_3 [19,20], and ureum [21,22]. There is no general agreement as to the nature of the active Cu sites in these catalysts, and the mechanism of NO and N_2O decomposition remains unclear [23–38]. In our previous work, we have proposed the existence of two types of active Cu sites: dimeric and monomeric [5,6]. Monomeric Cu sites are present in most Cu-containing zeolites. The reaction mechanism of N_2O decomposition is thought to consist of the deposition of oxygen atoms of N_2O onto the Cu sites, followed by recombination of two deposited oxygen atoms to molecular oxygen. This latter step involves migration of oxygen atoms over the catalyst surface [39]. At low Cu loading (Cu/Al < 0.28), the average Cu–Cu distance is large, and recombination is slow. The average Cu–Cu distance decreases with increasing Cu loading, as follows from the development of EPR-silent Cu. Accordingly, the rate of oxygen recombination is higher for catalysts with higher Cu loading [5]. Based on the results from a detailed spectroscopic study (UV–Vis and XAS) and after comparison with active sites in copper-containing proteins, the active site in Cu-ZSM-5 with high Cu loading (Cu/Al > 0.22) has been proposed to be a bis(μ-oxo)dicopper core [3,4,40,41]. The bridging oxygen atoms between the two Cu sites can originate from N_2O or NO. The close proximity of the oxygen species results in fast oxygen recombination, explaining the superior activity of Cu-ZSM-5 catalysts with high Cu loading [5].

Kinetic studies on N_2O decomposition have been reported for Cu-ZSM-5 and other transition-metal ions in ZSM-5 [42–44]. Besides the dependence of the activity on the Cu loading, we have found that the rate of N_2O decomposition also depends on the zeolite topology [5,6]. Consequently, comparing the kinetics of N_2O decomposition of a set of Cu-containing zeolites would appear to be of interest. We investigated 5 zeolite topologies (MFI, MOR, BEA, FER, and FAU) with low (Cu/Al < 0.28) and high (Cu/Al > 0.28) Cu loadings.

The effects of O_2, NO, and H_2O, which are typically present in tail gases of nitric acid plants requiring removal of N_2O, have been investigated previously, but no concise picture has emerged from these studies [30,42,43,45–48]. Most of the studies were performed using Cu-ZSM-5 with relatively high Cu loadings. Typically, NO has no effect or a negative effect on the catalytic N_2O decomposition. At low Cu loadings and with other Cu zeolites, NO has a beneficial effect on activity [5,6], as also has been reported for Fe-containing zeolites [49–57]. The mechanism in the latter case is

* Corresponding author. Fax: +32 16 321998.
E-mail address: robert.schoonheydt@biw.kuleuven.be (R.A. Schoonheydt).

0021-9517/$ – see front matter
doi:10.1016/j.jcat.2008.03.008

Table 1
Chemical and structural details of the catalysts

Sample[a]	Source	Topology	Si/Al	Cu/Al	Cu wt%
CuZSM-5(12–0.56)	ALSI-PENTA	MFI	12	0.56	4.3
CuZSM-5(12–0.42)	ALSI-PENTA	MFI	12	0.42	3.1
CuZSM-5(12–0.29)	ALSI-PENTA	MFI	12	0.29	2.3
CuZSM-5(12–0.22)	ALSI-PENTA	MFI	12	0.22	1.8
CuZSM-5(12–0.10)	ALSI-PENTA	MFI	12	0.10	0.9
CuMOR(5.3–0.39)	Norton	MOR	5.3	0.39	4.8
CuMOR(5.3–0.22)	Norton	MOR	5.3	0.22	2.7
CuMOR(8.8–0.50)	TRICAT	MOR	8.8	0.50	5.4
CuMOR(8.8–0.20)	TRICAT	MOR	8.8	0.20	2.1
CuFER(6.2–0.42)	Toyo Soda	FER	6.2	0.42	6.1
CuFER(6.2–0.21)	Toyo Soda	FER	6.2	0.21	3.1
CuBEA(9.8–0.38)	ZEOCAT™	BEA	9.8	0.38	2.8
Cu*Y*(2.7–0.47)	ZEOCAT™	FAU	2.7	0.47	10.6
Cu*Y*(2.7–0.28)	ZEOCAT™	FAU	2.7	0.28	6.9

[a] The samples are denoted as Cu*X*(*Y*–*Z*) were *X* stands for the zeolite, *Y* is the Si/Al ratio and *Z* the Cu/Al ratio.

explained in terms of NO scavenging of deposited oxygen atoms. Oxygen atoms are transported into the gas phase as NO_2, thus facilitating oxygen atom transport and recombination into molecular oxygen [58]. The influence of O_2 and H_2O on the N_2O decomposition activity of transition-metal ion-containing zeolites is negative [42,52,59–62]. In this paper, we report a surprising beneficial effect of the addition of water for catalysts with low Cu loading and for Cu-FAU catalysts.

2. Experimental

The origin and properties of the Cu-exchanged zeolites are collected in Table 1. The parent zeolites were first exchanged with Na^+ and then exchanged with Cu^{2+} as described previously [40,41]. The as-prepared samples are designated Cu*X*(*Y*–*Z*), where *X* represents the zeolite, *Y* is the Si/Al ratio, and *Z* is the Cu/Al ratio. The Cu and Al contents of the as-prepared zeolites were determined by inductively coupled plasma (ICP) after dissolution of the samples in HF.

Catalytic reaction experiments were performed in an automated parallel 10-flow microreactor setup. The catalyst was retained between two quartz wool plugs in a quartz reactor with an internal diameter of 4 mm. Each reactor was loaded with 0.2 g of catalyst with a sieve fraction of 0.25–0.5 mm. The standard pretreatment procedure consisted of heating the catalysts to 723 K at a rate of 1 K min^{-1} under a He flow of 50 ml min^{-1}. The decomposition of N_2O was subsequently carried out in a temperature-programmed mode by heating the catalysts from 573 to 823 K in steps of 10 K. The reactant feed (total flow, 1000 ml min^{-1}; 100 ml min^{-1} per catalyst) was composed by mixing appropriate flows of reaction gases through thermal mass flow controllers (Bronkhorst). Water was added through a liquid mass flow controller and a controlled evaporator mixer (CEM, Bronkhorst). Further details on the reaction setup are available elsewhere [5].

Analysis of effluent gases was done with a Balzers Omnistar mass spectrometer. The addition of small amounts of NO to N_2O did not affect accurate determination of the N_2O conversion [5]. Mass transport limitations in the catalyst bed were evaluated and could be excluded.

For CuZSM-5(12–0.56), an operando UV–Vis experiment was performed to study the effect of adding water during N_2O decomposition. The catalyst was continuously monitored by optical fiber UV–Vis spectroscopy in diffuse reflectance (DR) mode. A more detailed description of this setup is available elsewhere [2]. Before the experiment, the UV–Vis spectrum of a reactor containing Na-ZSM-5 was recorded and subsequently subtracted from the spectra of the Cu-ZSM-5 catalysts. Typically, 5000 scans were averaged in the 38,000–12,000 cm^{-1} region, with each scan taking 50 ms.

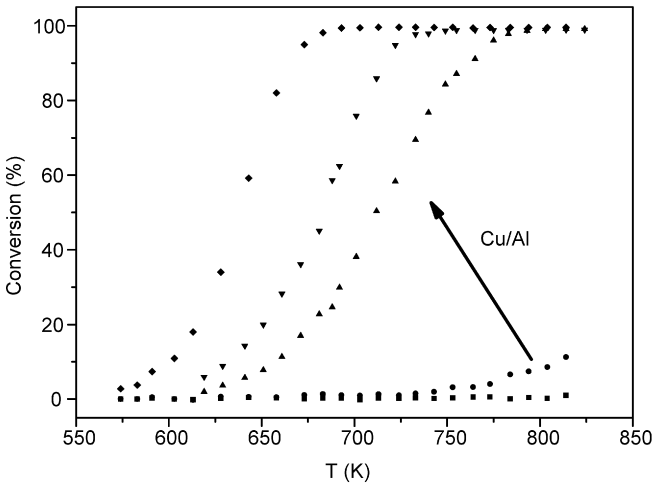

Fig. 1. Conversion of 1 vol% N_2O as a function of temperature for a Cu-ZSM-5 series with increasing Cu/Al ratio; ■ CuZSM-5(12–0.10), ● CuZSM-5(12–0.22), ▲ CuZSM-5(12–0.29), ▼ CuZSM-5(12–0.42), ◆ CuZSM-5(12–0.56).

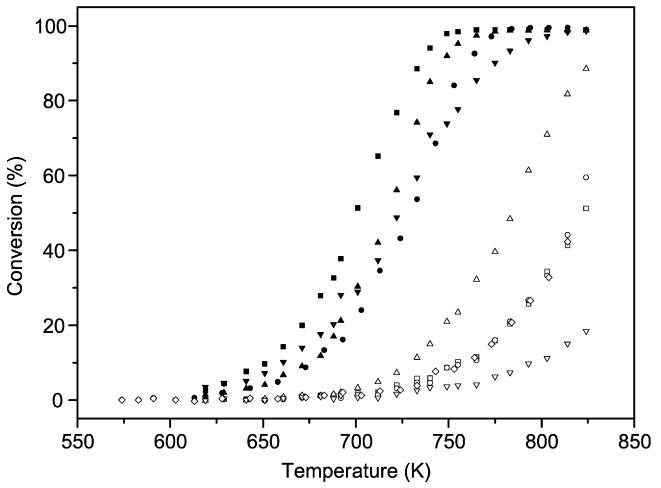

Fig. 2. Conversion of 1 vol% N_2O as a function of temperature for the other Cu-zeolites; ■ CuMOR(8.8–0.50), ● CuMOR(5.3–0.39), ▲ CuFER(6.2–0.42), ▼ Cu*Y*(2.7–0.47), □ CuMOR(8.8–0.20), ○ CuMOR(5.3–0.22), △ CuFER(6.2–0.21), ▽ Cu*Y*(2.7–0.28), ◇ CuBEA(9.8–0.38).

3. Results

3.1. Catalytic activity

The conversion of N_2O as a function of temperature for the various catalysts is shown in Fig. 1 (for the Cu-ZSM-5 series) and Fig. 2 (for the other zeolites). The most important observations that agree with earlier reports [2,3,5,6] are: (i) the superior activity of Cu-ZSM-5 catalysts with Cu/Al > 0.22; (ii) the very good performance of Cu-MOR, Cu-FER, and Cu–*Y* at high Cu loading (Cu/Al > 0.28); and (iii) the much lower activity of Cu-zeolites with low Cu/Al ratios irrespective of structure type.

Fig. 3 evaluates the effect of adding 5 vol% O_2, 0.1 vol% NO, and 5 vol% H_2O to the reactant feed for CuMOR(8.8–0.50) (Fig. 3a) and CuMOR(8.8–0.20) (Fig. 3b) as a function of temperature. Both figures reveal no significant effect of O_2 on the rate of N_2O decomposition. Adding 0.1 vol% NO lowered the T_{50} (i.e., temperature required for 50% conversion) by 20 K for CuMOR(8.8–0.50) and by 60 K for CuMOR(8.8–0.20). Similar trends were observed for the other zeolite topologies; a large temperature shift occurred for catalysts with low Cu loading (T_{50} decreased by 50–100 K), whereas a smaller shift was observed for catalysts with high Cu loading (T_{50}

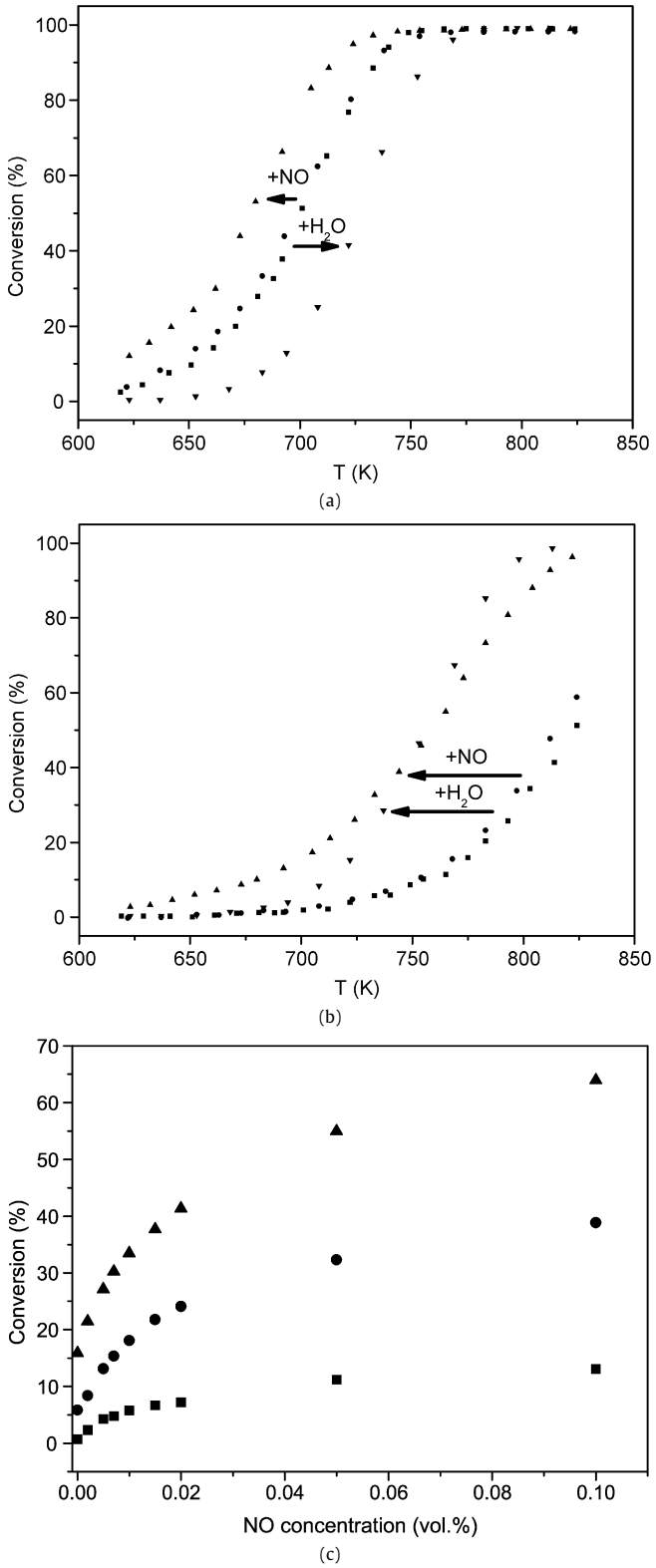

Fig. 3. (a) Conversion of N_2O over CuMOR(8.8–0.50) as a function of temperature: ■ 1 vol% N_2O, ● 1 vol% N_2O + 5 vol% O_2, ▲ 1 vol% N_2O + 0.1 vol% NO, ▼ 1 vol% N_2O + 5 vol% H_2O. (b) Conversion of N_2O over CuMOR(8.8–0.20) as a function of temperature: ■ 1 vol% N_2O, ● 1 vol% N_2O + 5 vol% O_2, ▲ 1 vol% N_2O + 0.1 vol% NO, ▼ 1 vol% N_2O + 5 vol% H_2O. (c) Conversion of 1 vol% N_2O over CuMOR(8.8–0.20) as a function of inlet NO concentration at ■ 693 K, ● 743 K, and ▲ 773 K.

decreased by <30 K). For CuZSM-5(12–0.56) and Cu*Y*(2.7–0.47), a negative effect of NO on conversion was observed, resulting in a <20 K increase in T_{50} (see Figs. S1–S12 in the Supporting Information). The effect of increasing the partial pressure of NO (from 0 to 0.1 vol%) for CuMOR(8.8–0.20) at 693, 743, and 773 K is shown in Fig. 3c. The conversion increased with the partial pressure of NO almost linearly up to about 0.01 vol% NO at all temperatures. At higher NO concentrations, the activity increase leveled off.

Table 2
Conversion of 1 vol% N_2O at: [a]703 K or [b]723 K before, during and 30 min after reaction with 5 vol% H_2O. In the last column, the shift in temperature to attain 50% conversion (T_{50}) before and during reaction with 5 vol% H_2O is given (+ means increased T_{50} in the presence of H_2O, − a decreased T_{50})

Sample	1 vol% N_2O	1 vol% N_2O + 5 vol% H_2O	1 vol% N_2O after 5 vol% H_2O	Shift in T_{50} (K)
CuZSM-5(12–0.56)[a]	100	31	100	+70
CuZSM-5(12–0.42)[b]	95	35	82	+40
CuZSM-5(12–0.29)[b]	58	20	45	+20
CuZSM-5(12–0.22)[a]	<1	4	2	−90[c]
CuZSM-5(12–0.10)[a]	<1	2	<1	−100[c]
CuMOR(5.3–0.39)[a]	24	13	34	+20
CuMOR(5.3–0.22)[b]	3	17	6	−70
CuMOR(8.8–0.50)[b]	77	42	74	+50
CuMOR(8.8–0.20)[b]	4	15	4	−60
CuFER(6.2–0.42)[b]	56	18	50	+30
CuFER(6.2–0.21)[b]	7	5	11	0
CuBEA(9.8–0.38)[a]	2	<1	<1	+60[d]
Cu*Y*(2.7–0.47)[b]	49	56	50	−10
Cu*Y*(2.7–0.28)[b]	2	22	4	−50[c]

[c] Estimated shift of T_{50} as the conversion of 1 vol% N_2O remained below 50% at temperatures up to 823 K in the absence of H_2O. In the presence of 5 vol% H_2O, 50% conversion was attained in the temperature range under investigation (see Figs. S1–S12 in the Supporting Information).

[d] Estimated shift of T_{50} as the conversion of 1 vol% N_2O remained below 50% at temperatures up to 823 K in the presence of 5 vol% H_2O. In the absence of H_2O, 50% conversion was attained in the temperature range under investigation (see Supporting Information).

Figs. 3a and 3b depict the effect of H_2O in the reactant feed on the N_2O conversion. For CuMOR(8.8–0.50), the activity clearly decreased in the presence of water (i.e., T_{50} increased by 50 K). For CuMOR(8.8–0.20), an opposite effect occurred; the addition of H_2O resulted in an increased conversion of N_2O (i.e., a 60 K decrease in T_{50}, from 823 to 763 K). Table 2 summarizes the shifts in T_{50} for the other catalysts. The data show that with increasing Cu loading, the positive effect of H_2O decreased and became negative for the catalysts with the highest Cu loadings (Cu/Al > 0.28). After 15 h on stream in a mixture of H_2O and N_2O, H_2O was removed from the reactant feed, and the activity of the various catalysts was measured after 30 min. The results are reported in Table 2. Clearly, the N_2O conversion was almost completely restored to its original value. This indicates that under the present reaction conditions, the effect of H_2O on N_2O decomposition was reversible.

The effect of H_2O was investigated in more detail for CuZSM-5(12–0.56), the catalyst with the highest activity in N_2O decomposition. Fig. 4 depicts the UV–Vis spectra of CuZSM-5(12–0.56) during direct N_2O decomposition at 673 K (Fig. 4a), during N_2O decomposition in the presence of H_2O at 673 K (Fig. 4b) and at 723 K (Fig. 4c), and during N_2O decomposition after H_2O treatment at 673 K (Fig. 4d). In the absence of H_2O, the spectra show the typical band at 22,000 cm^{-1}, ascribed to the Cu-dimer bridged by deposited oxygen atoms [2–5,40,41]. This band disappeared in the presence of H_2O, indicating the destruction of this active Cu dimer. This effect was fully reversible, however, as confirmed by the reappearance of the band at 22,000 cm^{-1} after removal of H_2O.

Fig. 5 shows the effect of calcination temperature on the activity in N_2O decomposition for CuZSM-5(12–0.56). On calcination at 1023 K, N_2O conversion was significantly reduced compared with that of the parent catalyst calcined at 723 K. In addition, NO demonstrated a beneficial effect on activity, in disagreement with our earlier finding for its parent counterpart [5]. Water, on

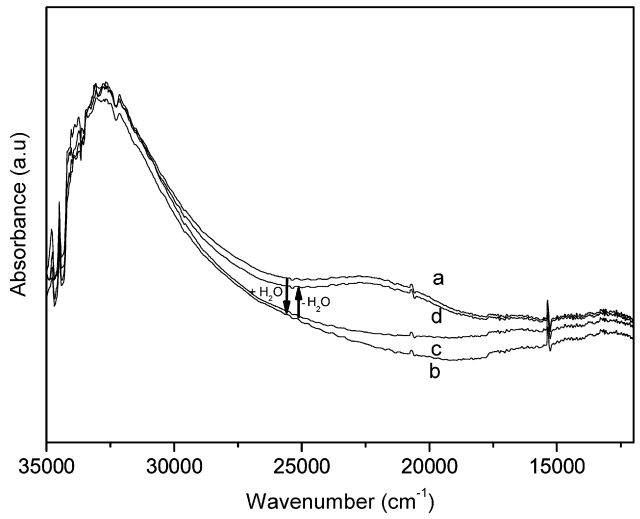

Fig. 4. Operando UV–Vis spectra of CuZSM-5(12–0.56) recorded during (a) 0.5 vol% N_2O at 673 K, (b) 0.5 vol% $N_2O + H_2O$ at 673 K, (c) 0.5 vol% $N_2O + H_2O$ at 723 K, (d) 0.5 vol% N_2O at 673 K 15 min after H_2O treatment.

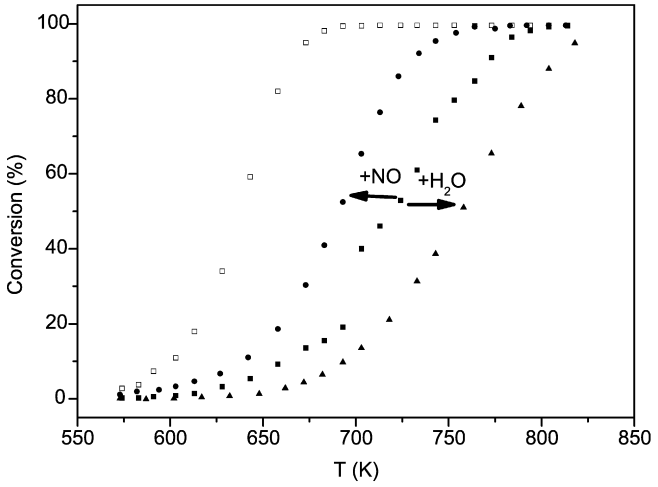

Fig. 5. Conversion of N_2O as a function of temperature for: □ CuZSM-5(12–0.56) calcined at 723 K during 1 vol% N_2O and for CuZSM-5(12–0.56) calcined at 1023 K during ■ 1 vol% N_2O, ● 1 vol% $N_2O + 0.1$ vol% NO, ▲ 1 vol% $N_2O + 5$ vol% H_2O.

the other hand had a negative effect, as also was observed after calcination at 723 K.

3.2. Kinetic evaluation

The apparent activation energies ($E_{act,app}$) were obtained from Arrhenius plots (see Supplementary Information, Fig. S13) and are collected in Table 3. Only the data points corresponding to conversion < 40% were taken into account. The values of $E_{act,app}$ for direct N_2O decomposition fell in the range of 110–150 kJ mol^{-1}. There was a tendency for higher values of the $E_{act,app}$ for catalysts with a lower Cu loading, but in most cases the differences were in the range of the experimental accuracy (±15 kJ mol^{-1}). Adding molecular oxygen to the reactant feed had no significant effect on $E_{act,app}$ (data not shown); however, adding NO resulted in a significant decrease in $E_{act,app}$ (typically, by 40–60 kJ mol^{-1}) for most of the Cu-containing zeolites. Only for Cu*Y*(2.7–0.47), CuFER(6.2–0.42), and the Cu-ZSM-5 zeolites with Cu/Al > 0.22 did the $E_{act,app}$ remain almost unchanged. The presence of 5 vol% H_2O resulted in an increase of $E_{act,app}$ of 50–80 kJ mol^{-1} (Table 3). For the Cu-*Y* zeolites, only a moderate increase in activation energy was observed (Table 3).

Table 3
Apparent activation energy in kJ mol^{-1} ($E_{act,app}$) during (i) the direct N_2O decomposition; (ii) the NO-assisted N_2O decomposition; (iii) N_2O decomposition under 5 vol% H_2O

Sample	$E_{act,app}$ 1 vol% N_2O	$E_{act,app}$ 1 vol% N_2O + 0.1 vol% NO	$E_{act,app}$ 1 vol% N_2O + 5 vol% H_2O
CuZSM-5(12–0.56)	130	123	194
CuZSM-5(12–0.42)	112	122	194
CuZSM-5(12–0.29)	125	118	195
CuZSM-5(12–0.22)	130	78	182
CuZSM-5(12–0.10)	n.a.	68	169
CuMOR(5.3–0.39)	129	94	179
CuMOR(5.3–0.22)	150	87	177
CuMOR(8.8–0.50)	122	85	195
CuMOR(8.8–0.20)	131	83	180
CuFER(6.2–0.42)	138	123	181
CuFER(6.2–0.21)	150	101	188
CuBEA(9.8–0.38)	145	83	177
Cu*Y*(2.7–0.47)	107	113	144
Cu*Y*(2.7–0.28)	127	92	122

Table 4
Order in N_2O at [a]693 K or [b]743 K during (i) the direct N_2O decomposition; (ii) the NO-assisted N_2O decomposition

Sample	Order in N_2O during direct N_2O	Order in N_2O during N_2O + 0.1 vol% NO
CuZSM-5(12–0.29)	0.7[a]	0.7[a]
CuZSM-5(12–0.22)	n.a.	0.7[a]
CuZSM-5(12–0.10)	n.a.	0.7[a]
CuMOR(5.3–0.39)	0.7[a]	0.7[a]
CuMOR(5.3–0.22)	0.4[b]	0.7[a]
CuMOR(8.8–0.50)	0.7[a]	n.a.
CuMOR(8.8–0.20)	0.4[b]	0.7[a]
CuFER(6.2–0.42)	0.7[a]	0.7[a]
CuFER(6.2–0.21)	0.6[b]	0.7[a]
CuBEA(9.8–0.38)	0.7[b]	0.7[a]
Cu*Y*(2.7–0.47)	0.7[a]	0.7[a]
Cu*Y*(2.7–0.28)	0.4[b]	0.9[a]

Fig. 6 plots reaction rates as a function of the concentration of N_2O for Cu-MOR catalysts in the absence of NO (Fig. 6a) and in the presence of 0.1 vol% NO (Fig. 6b). Here the slopes correspond to the reaction order in N_2O. The reaction orders for this catalyst and a number of others are given in Table 4. In direct N_2O decomposition, the order was 0.7, except at low Cu-loadings, in which case lower orders in N_2O of 0.6 [for CuFER(6.2–0.21)] and 0.4 [for CuMOR(5.3–0.22), CuMOR(8.8–0.20), and Cu*Y*(2.7–0.28)] were observed. In the presence of 0.1% NO, the order in N_2O was 0.7 for all catalysts, with a value of 0.9 for Cu*Y*(2.7–0.28).

4. Discussion

In the present work, kinetic data of the catalytic decomposition of N_2O were obtained and the effects of NO, O_2, and H_2O studied systematically. Based on the kinetic and catalytic data obtained, a reaction mechanism can be developed that demonstrates the importance of the recombinative O_2 desorption step for the overall activity.

4.1. Direct N_2O decomposition

Here the light-off temperature is defined as the temperature at which the conversion exceeds 5%. Taking this light-off temperature as a measure of activity in the decomposition of N_2O (see Figs. 1 and 2), the activity decreased in the following order, which corresponds well with our previous results [5,6]: Cu-ZSM-5 with Cu/Al > 0.22 (593–623 K, containing the active Cu-dimers) > other Cu MOR, FER, and *Y* catalysts with Cu/Al > 0.28 (623–673 K), containing a large fraction of EPR silent Cu sites ≫ Cu samples

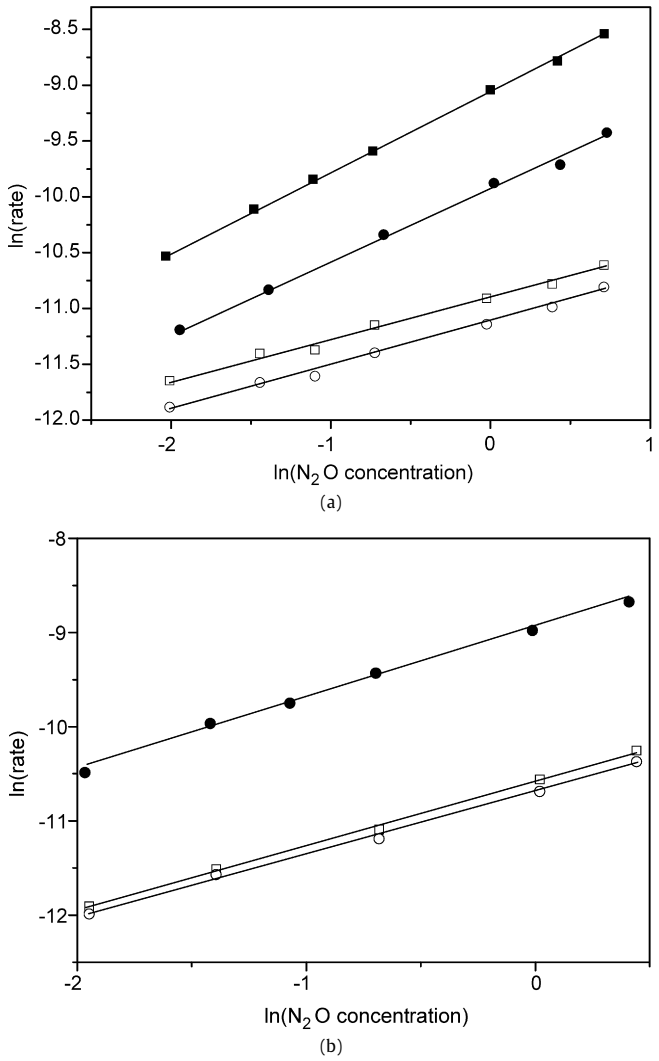

Fig. 6. (a) The ln(rate) as a function of ln(N_2O concentration) for ■ CuMOR(8.8–0.50) at 693 K, ● CuMOR(5.3–0.39) at 693 K, □ CuMOR(8.8–0.20) at 743 K, ○ CuMOR(5.3–0.22) at 743 K. (b) The ln(rate) as a function of ln(N_2O concentration) in the presence of 0.1 vol% NO at 693 K for ● CuMOR(5.3–0.39), □ CuMOR(8.8–0.20), ○ CuMOR(5.3–0.22).

with low Cu/Al ratios and CuBEA(9.8–0.38) (723–823 K; containing mostly isolated Cu sites). In previous work, we related the activity trends to differences in the distances that oxygen atoms must migrate [5] for oxygen recombination to occur. For catalysts in which Cu ions are relatively isolated (i.e., low Cu/Al ratios), the likelihood of oxygen recombination is low, and thus relatively high reaction temperatures are required (>723 K). When the Cu–Cu distance decreases with increasing Cu loading, the decreased distance between the deposited oxygen atoms leads to a significantly increased rate of recombination, and the reaction starts at 623–673 K. In the limiting case of formation of Cu dimers [2–5,40,41], activity is already observed below 623 K. It is interesting that the apparent activation energies do not differ considerably as a function of Cu loading, and thus the variations in activity are related to differences in the pre-exponential factor. To explore this in more detail, we assume that the rate is determined by recombinative oxygen desorption and that this is valid for all catalysts. In transition state theory, the rate is determined by the energy and entropy differences between the transition state and the ground state. The energy barrier is created largely through breakage of the Cu–O bond and formation of the O–O bond in the transition state. This difference likely will not depend strongly on the distance between the two Cu–O centers. In contrast, the entropy difference between the ground state and the transition state, as determined from the appropriate partition functions, depends strongly on the distance between the oxygen atoms. Thus, the pre-exponential factor will be larger when the oxygen atoms are proximate than when they are distant. This difference reflects the likelihood of formation of the transition state for oxygen desorption, which obviously decreases with increasing Cu–Cu distance.

4.1.1. Reaction mechanism over mononuclear Cu sites

Several reaction mechanisms have been proposed for the direct decomposition of N_2O over transition-metal ion-exchanged zeolites [42,61–67]. The first elementary reaction step is the chemisorption of an oxygen atom on an active Cu site (*) with concomitant release of N_2. For O_2 desorption, three steps can be envisaged: (i) recombinative desorption with a second oxygen atom (R2), (ii) direct reaction with gas-phase N_2O via an Eley-Rideal mechanism (R3), and (iii) after deposition of a second oxygen atom at the same site, that is, a single-site mechanism (R4):

$$N_2O + * \xrightarrow{k_2} N_2 + O^*, \quad \text{(R1)}$$

$$2O^* \xrightarrow{k_3} O_2 + 2^*, \quad \text{(R2)}$$

$$O^* + N_2O \rightarrow O_2 + N_2 + *, \quad \text{(R3)}$$

$$O^* + N_2O \rightarrow O_2{}^* + N_2 \rightarrow O_2 + *. \quad \text{(R4)}$$

Given the significant dependence of the activity in N_2O decomposition on the Cu loading and thus the average Cu–Cu distance, we concluded that the rate of the reaction is determined by the recombinative O_2 desorption [5]. Thus, (R2) is the most likely second reaction step, because neither an Eley-Rideal mechanism (R3) nor a single-site (R4) mechanism requires this migration. Moreover, experimentally the rate is independent of O_2 partial pressure (see below), and thus the reverse of (R2)—dissociative O_2 adsorption—can be neglected. In addition, (R4) can be ruled out, because inhibition by molecular oxygen is expected in a single-site mechanism (R4) [63]. Although the chemisorption of N_2O (R1) has been reported to be rate-determining in some cases [43,63], our results clearly show that the N_2O decomposition is limited by the recombinative desorption of O_2 (R2). Thus, the expression of the reaction rate is given by the following (see Supplementary Information):

$$r = k_3 N_{O^*}^2 = 2k_2 P_{N_2O} N_{Cu} - \frac{2}{k_3}(k_2 P_{N_2O})^2 \left(\sqrt{1 + 2N_{Cu}\frac{k_3}{k_2 P_{N_2O}}} - 1 \right). \quad \text{(RE1)}$$

Here N_{Cu} equals the sum of empty Cu sites (N_*) and Cu sites covered with O atoms (N_{O^*}). If all of the Cu ions are accessible for N_2O, then N_{Cu} equals the total Cu content. This certainly is not the case for Cu-*Y* zeolites, however, in which a large fraction of Cu ions are located inside the sodalite cages, making them inaccessible and unavailable for reaction [6,68]. At high Cu loading, the reaction rate increases due to a decreasing Cu–Cu distance. This is expressed by an increased amount of EPR-silent Cu species [5]. As an approximation, the latter can be taken as N_{Cu} in equation (RE1).

In Eq. (RE1) we may assume that $k_3 < k_2$, because (R2) is rate-determining. In the limit of extremely small k_3, all Cu sites are occupied by oxygen atoms, and N_{O^*} equals N_{Cu}. Thus (RE1) becomes (RE1′):

$$r = k_3 N_{Cu}^2. \quad \text{(RE1′)}$$

The rate is independent of the partial pressure of N_2O, and the order in N_2O is zero. As k_3 increases, the empty sites (N_*) should be accounted for, and the order in N_2O should increase, as evidenced by (RE1). Oxygen atom recombination speeds up as the distance

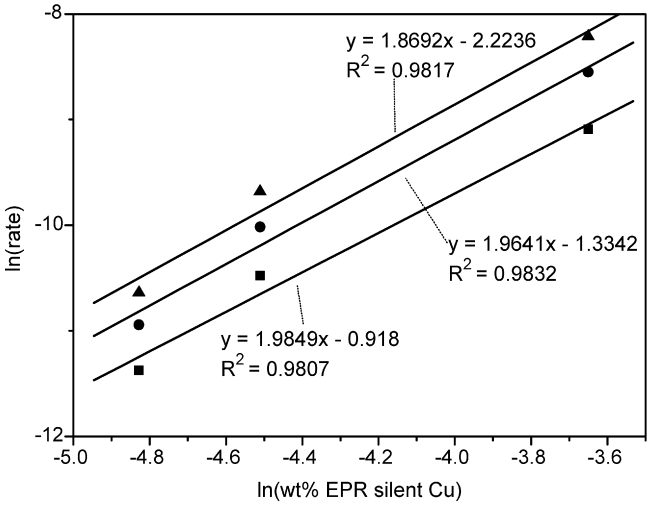

Fig. 7. The ln(rate) as a function of ln(EPR silent Cu wt%) of CuZSM-5(12–0.29), CuZSM-5(12–0.42) and CuZSM-5(12–0.56) at ■ 623 K, ● 633 K, and ▲ 643 K. The equation for the linear fit, as well as the R^2 is given for each temperature.

between the Cu sites decreases, that is, at higher Cu loading; thus, k_3 increases with increasing Cu loading, and the order in N_2O will increase accordingly. From Table 4, we indeed observe a lower order in N_2O for the catalysts with Cu/Al < 0.28 compared to the catalysts with higher Cu/Al ratios (0.4 vs 0.7).

4.1.2. Reaction mechanism over dinuclear Cu sites (Cu-ZSM-5 with Cu/Al>0.22)

The superior activity of CuZSM-5(12–0.56) in N_2O decomposition is attributed to the presence of Cu dimers bridged by two deposited oxygen atoms, from which molecular oxygen can desorb without an oxygen migration step. Groothaert et al. [2,3] proposed the following mechanism for the direct decomposition of N_2O over these Cu dimers (R1*)–(R4*):

$$^{**} + N_2O \xrightarrow{k_2} {}^{*}O^{*} + N_2, \quad \text{(R1*)}$$

$$^{*}O^{*} + N_2O \xrightarrow{k_{2'}} {}^{*}OO^{*} + N_2, \quad \text{(R2*)}$$

$$^{*}OO^{*} \xrightarrow{k_3} {}^{**} + O_2, \quad \text{(R3*)}$$

$$^{*}OO^{*} + N_2O \xrightarrow{k_{3'}} {}^{*}O^{*} + O_2 + N_2. \quad \text{(R4*)}$$

Because O_2 inhibition is not observed (see Figs. S3–S5 in Supplementary Information), the reverse of reactions (R3*) and (R4*) are not accounted for. Desorption of molecular oxygen is the rate-limiting step, because the temperature of formation of the dimer cores is lower than the decomposition temperature of these cores [41]. This results in the following rate expression:

$$r = k_3 N_{*_{OO^*}} + k_{3'} N_{*_{OO^*}} P_{N_2O} = (k_3 + k_{3'} P_{N_2O}) N_{*_{OO^*}}$$
$$= (k_3 + k_{3'} P_{N_2O}) \frac{k_2 k_{2'} P_{N_2O}}{k_3 k_{2'} + k_2 k_3 + k_2 P_{N_2O} (k_{2'} + k_{3'})} N_{CuCu}, \quad \text{(RE2)}$$

where N_{CuCu} represents the total amount of active dimers present in Cu-ZSM-5. Because the Cu dimers are formed from two neighboring EPR-silent Cu atoms [3], a second-order dependence of the reaction rate in EPR-silent Cu atoms is expected. Fig. 7 plots the dependence of the reaction rate as a function of the concentration of EPR-silent Cu ions [5] for CuZSM-5(12–0.29), CuZSM-5(12–0.42), and CuZSM-5(12–0.56) at various temperatures. The reaction order in EPR-silent Cu is close to 2 (slope of the curves, 1.87–1.91). Despite the fact that we have results for only three different samples (with different Cu wt% points), and thus these results must be interpreted with care, these findings support the assignment of this Cu dimer as the active site.

The mechanism of formation of these dinuclear sites in ZSM-5 remains unclear and is very peculiar in any case. The active dimers are no longer formed after calcination at temperatures above 973 K [41]. Fig. 5 shows that the activity decreases significantly after this high-temperature pretreatment, confirming the assignment of these Cu dimers as the sites responsible for the superior activity of CuZSM-5(12–0.56). Adding NO results in increased N_2O conversion over the CuZSM-5(12–0.56) catalyst calcined at 1023 K, in contrast to the effect for the parent catalysts calcined at 723 K. This indicates a change in mechanism and suggests the involvement of an oxygen migration step in the decomposition of N_2O once the catalyst is calcined at temperatures above 973 K.

4.2. Effect of NO

NO scavenges deposited O atoms (R5) and transports them into the gas phase as NO_2 (R6). O_2 is released from NO_2 either via the reaction with a second deposited oxygen atom (R7) or via the gas-phase reaction with a second NO_2 molecule (R8). In this way, oxygen migration over single Cu sites is complemented by oxygen atom migration in the gas phase. The effect is most pronounced at low Cu/Al ratios (>50 K decrease in T_{50}), that is, when the average distance between the Cu sites is large. As the Cu content of the catalyst increases, (R2) becomes more competitive with (R5)–(R8), and the positive effect of NO diminishes (<30 K decrease in T_{50}; see Fig. 3) [5,6]. As a result, the order in N_2O is comparable (0.7) at low and high Cu loadings (Table 4). In addition, at low Cu loading, the $E_{act,app}$ is decreased significantly due to the predominance of (R5)–(R8):

$$O^{*} + NO \leftrightarrow NO_2{}^{*}, \quad \text{(R5)}$$

$$NO_2{}^{*} \leftrightarrow NO_2 + {}^{*}, \quad \text{(R6)}$$

$$NO_2 + O^{*} \rightarrow NO + O_2 + {}^{*}, \quad \text{(R7)}$$

$$2NO_2 \leftrightarrow 2NO + O_2. \quad \text{(R8)}$$

Fig. 3c shows that the conversion of N_2O increases linearly with increasing NO concentration up to 0.01 vol% NO, then levels off at higher NO vol%. This can be attributed to the higher steady-state concentration of NO_2; the specific dependence suggests an equilibrium between NO in the gas phase and adsorbed NO according to a Langmuir adsorption model. The rate-limiting step is then the reaction of gas-phase NO_2 (in equilibrium with adsorbed NO_2) with surface oxygen atoms (R7) or with another gas-phase NO_2 molecule (R8) [5].

4.3. Effect of O_2

In the present work, we see that the molecular recombination of oxygen atoms to molecular oxygen is a rate-determining step. This agrees with reports for other transition-metal-containing zeolites [64]. But, as follows from Figs. 3a and 3b, O_2 has no effect on the rate of N_2O decomposition. Because the deposited oxygen atoms must migrate before recombinative O_2 desorption can occur, it seems plausible to posit that the absence of O_2 inhibition is related to the very low rate of the reverse reaction (dissociative O_2 chemisorption). This low rate is associated with the higher bond energy of O_2 (498 kJ mol^{-1}) compared to the N–O bond in N_2O (167 kJ mol^{-1}) [69] and the large loss in entropy associated with dissociation of molecular oxygen over distant Cu sites instead of the deposition of one oxygen atom from N_2O. Indeed, we find that even for Cu-ZSM-5, the formation of the Cu dimers bridged by two oxygen atoms proceeds at appreciably lower temperature with N_2O as an oxidant than with O_2 as an oxidant (unpublished results). A similar lack of inhibition of molecular oxygen also has been observed for Fe-ZSM-5 [61,65,66].

4.4. Effect of H_2O

The promotion of catalytic activity by H_2O for MOR, FER, and ZSM-5 catalysts containing predominantly isolated Cu sites (Cu/Al < 0.25) has not been reported previously. For the zeolite *Y*-based catalysts, a beneficial effect of water is noted at both high and low Cu loadings. Table 2 summarizes the changes in activity, in terms of T_{50}, due to the addition of H_2O. As an example, CuZSM-5(12–0.10), which exhibits no activity in direct N_2O decomposition in the temperature range under investigation (573–823 K), becomes quite active at 823 K (62%) in the presence of water (see Supplementary Information, Fig. S1). To the best of our knowledge, no such significant beneficial effect of H_2O has been reported for the catalytic decomposition of N_2O [70–73].

The literature contains numerous reports of polar molecules, like H_2O, inducing reversible migration of transition-metal ions in zeolites [21,46,68,74–76]. Our work shows that the activity of proximate Cu centers is much higher than that of highly isolated Cu centers. The positive effect of water for isolated, distantly placed Cu ions thus suggests that the distance between Cu sites decreases due to the migration of hydrated Cu atoms. Such hydrated Cu ions may be expected to not contribute to catalytic activity, but if this is so, then transiently vacant Cu sites will be present, because adsorbed water is in equilibrium with gas-phase water. Thus, oxygen atoms can be deposited closer to one another, facilitating oxygen recombination. The beneficial effect of water over Cu-zeolites with low Cu loading is tentatively assigned to water-induced migration of Cu ions. In Cu-*Y*, a beneficial effect of H_2O on the conversion of N_2O is observed at all Cu loadings investigated (Table 2 and Figs. S11 and S12 in Supplementary Information). In these catalysts, a large fraction of Cu atoms are located in the sodalite cages and thus are inaccessible for the catalytic conversion of N_2O [6,68, 77–81]. In the presence of H_2O, these ions partially migrate to the supercages [68,82]; thus, the number of catalytically active Cu ions increases, as does the reaction rate. This mechanism provides a reasonable explanation for the increased activity of the Cu-*Y* samples even at high Cu loading.

For the other Cu-zeolites, a negative effect of H_2O on the N_2O decomposition is observed at Cu/Al > 0.25, in agreement with literature data [52,60–62,65,71,83–88]. This negative effect of H_2O is most often attributed to competitive adsorption between N_2O and H_2O. This would seem to agree with the increase in the apparent activation energies compared with those of dry N_2O decomposition (Table 3). The value of $E_{act,app}$ depends on the heat of adsorption of the various surface species, and competitively adsorbed water will increase the measured activation energy. The overall effect of water on N_2O decomposition thus appears to be a combination of competitive adsorption, resulting in an increased $E_{act,app}$, and a redistribution of Cu ions, resulting in a decreased Cu–Cu distance and more facile oxygen recombination. At high Cu loading, the effect of competitive adsorption dominates, leading to decreased catalytic activity. For catalysts with relatively low Cu loading (Cu/Al < 0.25), the decreased Cu–Cu distance results in more facile oxygen migration and significantly increased catalytic activity. This effect predominates over the negative effect of competitive adsorption. To obtain better insight into these effects as a function of the Cu/Al ratio, Fig. 8 plots the activity per Cu atom (TOF) for CuMOR(8.8–0.50) and CuMOR(8.8–0.20) in the absence (Fig. 8a) and presence (Fig. 8b) of 5 vol% H_2O. Whereas in the absence of H_2O, CuMOR(8.8-0.50) has a higher TOF than CuMOR(8.8–0.20), in the presence of H_2O, the two samples have almost equal TOFs. In addition, the difference in light-off temperature between the two samples is much smaller in the presence of H_2O than in the absence of H_2O; the light-off temperature of CuMOR(8.8–0.50) increases by 50 K, whereas that of CuMOR(8.8–0.20) decreases by 50 K. The similar TOFs and light-off temperatures indicate that the activity of Cu sites is independent of the Cu loading in the presence of H_2O.

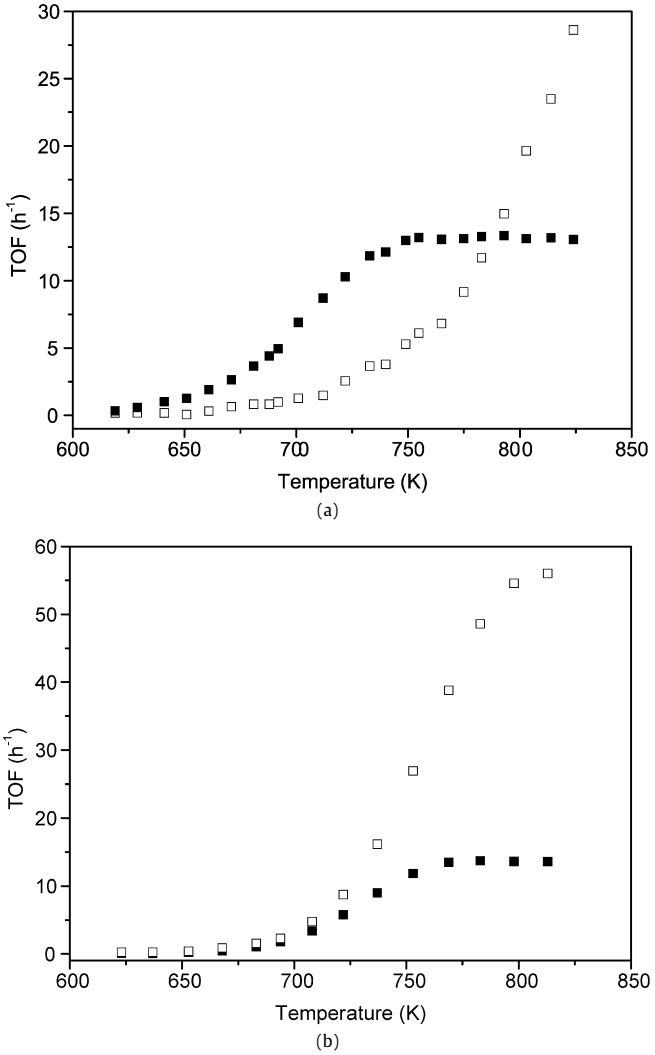

Fig. 8. (a) Turn-over frequency (h^{-1}) during 1 vol% N_2O decomposition as a function of temperature for ■ CuMOR(8.8–0.50) and □ CuMOR(8.8–0.20). (b) Turn-over frequency (h^{-1}) during 1 vol% N_2O decomposition in the presence of 5 vol% H_2O as a function of temperature for ■ CuMOR(8.8–0.50) and □ CuMOR(8.8–0.20). At temperatures higher than 723 K, conversion over CuMOR(8.8–0.50) exceeds 50% explaining the leveling off of the TOFs at these temperatures.

The only exception to this finding in the present study is zeolite BEA. In CuBEA(9.8–0.38), which contains mostly isolated Cu sites [5], an increase in activity after addition of H_2O would be expected; however, as shown in Table 2 (and Fig. S10 in Supplementary Information), H_2O actually has a negative effect on N_2O conversion. A similar negative effect was observed for a BEA sample with low Cu/Al ratio (CuBEA(9.8–0.17) from [5], results not shown). Recent studies have reported a less-pronounced mobility of transition-metal ions in BEA [89], explaining why the effect of competitive adsorption of H_2O prevails [90,91] and produces an overall negative effect in the Cu-BEA samples, even at isolated Cu sites.

The operando UV–Vis spectra of CuZSM-5(12–0.56) recorded during H_2O treatment (Fig. 4) show that the addition of H_2O results in the disappearance of the band at 22,700 cm^{-1}, that is, the absorption band originating from the oxygen-bridged Cu dimers. In earlier work, we attributed the extreme sensitivity of this core to H_2O [3,40,41]. The disappearance of the Cu dimer signal may be related to the strong coordination of water to Cu ions. Thus, it

is reasonable to assume that the lower activity in the presence of water is related to a decreased number of Cu dimers. But the effect of water is completely reversible, as indicated by the complete restoration of the typical band at 22,700 cm^{-1} on removal of water from the feed (Fig. 4d). The activity results (Table 2) confirm the reversible nature of the effect of H_2O. This implies that water does not induce drastic structural changes as are caused by sintering or dealumination of the zeolite framework [60,65,89,92,93]. Thus, the Cu-containing zeolites exhibit good stability under the present reaction conditions.

5. Conclusion

Deposition of oxygen atoms on the active Cu sites (R1) and recombination to molecular oxygen (R2) are the key steps in the catalytic decomposition of N_2O over Cu-containing zeolites. Based on our previous results [5] and the present findings, we can conclude that (R2) is the rate-limiting step, resulting in an expression for the reaction rate in (RE1). In this expression, the importance of the rate of O recombination through migration over the surface (k_3) is shown, demonstrating how the distance between monomeric Cu sites affects the activity and reaction order in N_2O (EPR-silent vs isolated Cu sites). In Cu-ZSM-5 with high Cu loading (Cu/Al $>$ 0.25), the decomposition of N_2O occurs over dimeric Cu sites, making the oxygen migration step obsolete. O_2 desorption remains the rate-limiting step at these dimeric sites. The activity in N_2O decomposition is greatly reduced after high-temperature calcination of CuZSM-5(12–0.56), which is known to result in the disappearance of active Cu dimers [41]. This finding confirms that these dimers are responsible for the superior activity of Cu-ZSM-5. An expression for the reaction rate over these cores, calculated in (RE2), suggests a second order in EPR-silent Cu, which was confirmed by the catalytic results.

NO intervenes in the catalytic N_2O decomposition by providing an alternative route for oxygen migration via gaseous NO_2. Its effect is greatest for catalysts with low Cu loading and results in an increased order in N_2O and a decreased $E_{act,app}$ over these catalysts. At high NO partial pressure, the rate-limiting step is the release of O_2 from this gaseous intermediate. The rate of N_2O decomposition is not dependent on the partial pressure of molecular oxygen, indicating that dissociative O_2 adsorption is much slower than recombinative O_2 desorption.

Water has two opposing effects on the rate of N_2O decomposition: competitive adsorption of H_2O on the active Cu site, resulting in an increased $E_{act,app}$, and a redistribution of Cu ions. The former effect dominates over ZSM-5, MOR, FER, and BEA catalysts with high Cu loading (Cu/Al $>$ 0.25) and leads to a decreased reaction rate. The operando UV–Vis study demonstrates that for Cu-ZSM-5, the Cu-dimers are not stable in the presence of water; tentatively, this may be explained by the stronger coordination of water compared with N_2O. For Cu-containing zeolites of the ZSM-5, MOR, and FER topology and with Cu/Al $<$ 0.25, the activity increases significantly. In all cases, the apparent activation energy increases when water is added to the reaction feed. This is in line with a kinetic model in which water competitively adsorbs for the Cu sites with N_2O; the apparent activation energy increases by an amount proportional to the water surface coverage and the adsorption energy of water. Clearly, for the catalysts with a low Cu/Al ratio, the effect of Cu migration appears to dominate over the effect of competitive water adsorption. For Cu-*Y* catalysts, we surmise that removal of Cu atoms from the inaccessible sodalite cages increases the number of catalytically active Cu ions. This explains the beneficial effect of water for Cu-*Y*, even at a high Cu loading. Removing water from the reaction feed restores the original activity levels; thus, it can be concluded that the effect of water is fully reversible.

Acknowledgments

This investigation was supported by grants from the Concerted Research Action (G.O.A.), the Interuniversity Attraction Pool (IAP) program, the Centre of Excellence at the University of Leuven (CECAT), and the European Centre of Excellence Network (IDECAT). P.J.S. thanks the Institute for the Promotion of Innovation through Science and Technology in Flanders (I.W.T.-Vlaanderen) for a PhD grant.

Supporting information

The online version of this article contains additional supporting information.

Please visit doi: 10.1016/j.jcat.2008.03.008.

References

[1] M. Iwamoto, H. Yahiro, K. Tanda, N. Mizuno, Y. Mine, S. Kagawa, J. Phys. Chem. 95 (1991) 3727.
[2] M.H. Groothaert, K. Lievens, H. Leeman, B.M. Weckhuysen, R.A. Schoonheydt, J. Catal. 220 (2003) 500.
[3] M.H. Groothaert, J.A. van Bokhoven, A.A. Battiston, B.M. Weckhuysen, R.A. Schoonheydt, J. Am. Chem. Soc. 125 (2003) 7629.
[4] M.H. Groothaert, K. Lievens, J.A. van Bokhoven, A.A. Battiston, B.M. Weckhuysen, K. Pierloot, R.A. Schoonheydt, ChemPhysChem 4 (2003) 626.
[5] P.J. Smeets, M.H. Groothaert, R.M. van Teeffelen, H. Leeman, E.J.M. Hensen, R.A. Schoonheydt, J. Catal. 245 (2007) 358.
[6] P.J. Smeets, M.H. Groothaert, R.M. van Teeffelen, H. Leeman, E.J.M. Hensen, R.A. Schoonheydt, Stud. Surf. Sci. Catal. 170 (2007) 1080.
[7] J. Pérez-Ramirez, Patent WO047960A1 (2004), to Norsk Hydro asa.
[8] B. Modén, P. Da Costa, B. Fonfé, D.K. Lee, E. Iglesia, J. Catal. 209 (2002) 75.
[9] M.Y. Kustova, S.B. Rasmussen, A.L. Kustov, C.H. Christensen, Appl. Catal. B 67 (2006) 60.
[10] M.Y. Kustova, A. Kustov, S.E. Christiansen, K.T. Leth, S.B. Rasmussen, C.H. Christensen, Catal. Commun. 7 (2006) 705.
[11] J. Dedecek, O. Bortnovsky, A. Vondrová, B. Wichterlová, J. Catal. 200 (2001) 160.
[12] J. Dedecek, J. Cejka, B. Wichterlová, Appl. Catal. B 15 (1998) 233.
[13] A.T. Bell, Catal. Today 38 (1997) 151.
[14] P.E. Fanning, M.A. Vannice, J. Catal. 207 (2002) 166.
[15] M. Shimokawabe, K. Hirano, N. Takezawa, Catal. Today 45 (1998) 117.
[16] P. Pietrzyk, B. Gil, Z. Sojka, Catal. Today 126 (2007) 103.
[17] R.S. da Cruz, A.J.S. Mascarenhas, H.M.C. Andrade, Appl. Catal. B 18 (1998) 223.
[18] N.W. Cant, I.O.Y. Liu, Catal. Today 63 (2000) 133.
[19] H. Sjövall, L. Olsson, E. Fridell, R.J. Blint, Appl. Catal. B 64 (2006) 180.
[20] G. Busca, M.A. Larrubia, L. Arrighi, G. Ramis, Catal. Today 107–108 (2005) 139.
[21] J. Park, H.J. Park, J.H. Baik, I. Nam, C. Shin, J. Lee, B.K. Cho, S.H. Oh, J. Catal. 240 (2006) 47.
[22] L. Xu, R.W. McCabe, R.H. Hammerle, Appl. Catal. B 39 (2002) 51.
[23] M.H. Groothaert, K. Pierloot, A. Delabie, R.A. Schoonheydt, Phys. Chem. Chem. Phys. 5 (2003) 2135.
[24] A. Delabie, K. Pierloot, M.H. Groothaert, B.M. Weckhuysen, R.A. Schoonheydt, Phys. Chem. Chem. Phys. 4 (2002) 134.
[25] S.A. Yashnik, Z.R. Ismagilov, V.F. Anufrienko, Catal. Today 110 (2005) 310.
[26] Z. Schay, L. Guczi, A. Beck, I. Nagy, V. Samuel, S.P. Mirajkar, A.V. Ramaswamy, G. Pál-Borbély, Catal. Today 75 (2002) 393.
[27] P.T. Fanson, M.W. Stradt, J. Lauterbach, W.N. Delgass, Appl. Catal. B 38 (2002) 331.
[28] T. Ochs, T. Turek, Chem. Eng. Sci. 54 (1999) 4513.
[29] L. Chen, H.Y. Chen, J. Lin, K.L. Tan, Surf. Interface Anal. 28 (1999) 115.
[30] T. Turek, J. Catal. 174 (1998) 98.
[31] P. Da Costa, B. Modén, G.D. Meitzner, D.K. Lee, E. Iglesia, Phys. Chem. Chem. Phys. 4 (2002) 4590.
[32] R. Bulánek, P. Cicmanec, P. Knotek, D. Nachtigallová, P. Nachtigall, Phys. Chem. Chem. Phys. 6 (2004) 2003.
[33] B.F. Mentzen, G. Bergeret, J. Phys. Chem. C 111 (2007) 12512.
[34] B.R. Goodman, K.C. Hass, W.F. Schneider, J.B. Adams, J. Phys. Chem. B 103 (1999) 10452.
[35] D. Berthomieu, S. Krishnamurty, B. Coq, G. Delahay, A. Goursot, J. Phys. Chem. B 105 (2001) 1149.
[36] N. Jardillier, D. Berthomieu, A. Goursot, J.U. Reveles, A.M. Koster, J. Phys. Chem. B 110 (2006) 18440.
[37] B.R. Goodman, W.F. Schneider, K.C. Hass, J.B. Adams, Catal. Lett. 56 (1998) 183.
[38] V. Petranovskii, V. Gurin, R. Machorro, Catal. Today 107–108 (2005) 892.
[39] J. Valyon, W.S. Millman, W.K. Hall, Catal. Lett. 24 (1994) 215.
[40] M.H. Groothaert, P.J. Smeets, B.F. Sels, P.A. Jacobs, R.A. Schoonheydt, J. Am. Chem. Soc. 127 (2005) 1394.

[41] P.J. Smeets, M.H. Groothaert, R.A. Schoonheydt, Catal. Today 110 (2005) 303.
[42] F. Kapteijn, G. Marbán, J. Rodriguez-Mirasol, J.A. Moulijn, J. Catal. 167 (1997) 256.
[43] A. Dandekar, M.A. Vannice, Appl. Catal. B 22 (1999) 179.
[44] P. Ciambelli, A. Di Benedetto, R. Pirone, G. Russo, Chem. Eng. Sci. 54 (1999) 2555.
[45] G. Centi, A. Galli, B. Montanari, S. Perathoner, A. Vaccaria, Catal. Today 35 (1997) 113.
[46] S.A. Gómez, A. Campero, A. Martínez-Hernández, G.A. Fuentes, Appl. Catal. A 197 (2000) 157.
[47] F.X. Llabres i Xamena, P. Fisicaro, G. Berlier, A. Zecchina, G.T. Palomino, C. Prestipino, S. Bordiga, E. Giamello, C. Lamberti, J. Phys. Chem. B 107 (2003) 7036.
[48] G.T. Palomino, P. Fisicaro, E. Giamello, S. Bordiga, C. Lamberti, A. Zecchina, J. Phys. Chem. B 104 (2000) 4064.
[49] G. Mul, J. Pérez-Ramírez, F. Kapteijn, J.A. Moulijn, Catal. Lett. 77 (2001) 7.
[50] M. Kögel, B.M. Abu-Zied, M. Schwefer, T. Turek, Catal. Commun. 2 (2001) 273.
[51] J. Pérez-Ramírez, F. Kapteijn, G. Mul, J.A. Moulijn, J. Catal. 208 (2002) 211.
[52] X. Xu, H. Xu, F. Kapteijn, J.A. Moulijn, Appl. Catal. B 53 (2004) 265.
[53] I. Melián-Cabrera, C. Mentruit, J.A.Z. Pieterse, R.W. van den Brink, G. Mul, F. Kapteijn, J.A. Moulijn, Catal. Commun. 6 (2005) 301.
[54] J.A.Z. Pieterse, G. Mul, I. Melian-Cabrera, R.W. Brink, Catal. Lett. 99 (2005) 41.
[55] C. Sang, B.H. Kim, C.R.F. Lund, J. Chem. Phys. B 109 (2005) 2295.
[56] D. Kaucký, Z. Sobalík, M. Schwarze, A. Vondrová, B. Wichterlová, J. Catal. 238 (2006) 293.
[57] G.D. Pirngruber, J.A.Z. Pieterse, J. Catal. 237 (2006) 237.
[58] B. Moden, P. Da Costa, D.K. Lee, E. Iglesia, J. Phys. Chem. B 106 (2002) 9633.
[59] J. Pérez-Ramírez, F. Kapteijn, G. Mul, J.A. Moulijn, Appl. Catal. B 35 (2002) 227.
[60] D.A. Bulushev, P.M. Prechtl, A. Renken, L. Kiwi-Minsker, Ind. Eng. Chem. Res. 46 (2007) 4178.
[61] A. Heyden, B. Peters, A.T. Bell, F.J. Keil, J. Phys. Chem. B 109 (2005) 1857.
[62] A. Heyden, A.T. Bell, F.J. Keil, J. Catal. 233 (2005) 26.
[63] L. Obalova, V. Fila, Appl. Catal. B 70 (2007) 353.
[64] E.V. Kondratenko, J. Pérez-Ramirez, J. Phys. Chem. B 110 (2006) 22586.
[65] F. Kapteijn, J. Rodriguez-Mirasol, J.A. Moulijn, Appl. Catal. B 9 (1996) 25.
[66] G.D. Pirngruber, P.K. Roy, R. Prins, J. Catal. 246 (2007) 147.
[67] D. Sengupta, J.B. Adams, W.F. Schneider, K.C. Hass, Catal. Lett. 74 (2001) 193.
[68] G.T. Palomino, S. Bordiga, A. Zecchina, G.L. Marra, C. Lamberti, J. Chem. Phys. B 104 (2000) 8641.
[69] D.R. Lide, Handbook of Chemistry and Physics, CRC Press, London, 2004, pp. 9–56.
[70] H. Chen, W.M.H. Sachtler, Catal. Today 42 (1998) 73.
[71] C. Descorme, P. Gélin, C. Lécuyer, M. Primet, J. Catal. 177 (1998) 352.
[72] L. Capek, K. Novoveska, Z. Sobalík, B. Wichterlova, L. Cider, E. Jobson, Appl. Catal. B 60 (2005) 201.
[73] L. Capek, L. Vradman, P. Sazama, M. Herskowitz, B. Wichterlova, R. Zukerman, R. Brosius, J.A. Martens, Appl. Catal. B 70 (2007) 53.
[74] A.V. Kucherov, H.G. Karge, R. Schlögl, Microporous Mesoporous Mater. 25 (1998) 7.
[75] M.W. Anderson, L. Kevan, J. Phys. Chem. 91 (1987) 4174.
[76] A. Zecchina, S. Bordiga, G.T. Palomino, D. Scarano, C. Lamberti, M. Salvalaggio, J. Phys. Chem. B 103 (1999) 3833.
[77] W.J. Mortier, Compilation of Extra Framework Sites in Zeolites, Butterworth Scientific Ltd., Guildford, 1982, p. 621.
[78] P. Gallezot, Y. Ben Taarit, B. Imelik, J. Catal. 26 (1972) 295.
[79] C.O. Kowenje, B.R. Jones, D.C. Doetschman, S. Yang, C.W. Kanyi, Chem. Phys. 330 (2006) 401.
[80] K. Pierloot, A. Delabie, M.H. Groothaert, R.A. Schoonheydt, Phys. Chem. Chem. Phys. 3 (2001) 2174.
[81] P. Rejmak, M. Sierka, J. Sauer, Phys. Chem. Chem. Phys. 9 (2007) 5446.
[82] D. Berthomieu, N. Jardillier, G. Delahay, B. Coq, A. Goursot, Catal. Today 110 (2005) 294.
[83] M. Shimokawabe, H. Ono, S. Sasaki, N. Takezawa, Appl. Surf. Sci. 121–122 (1997) 400.
[84] A. Frache, B.I. Palella, M. Cadoni, R. Pirone, H.O. Pastore, L. Marchese, Top. Catal. 22 (2003) 53.
[85] B.I. Palella, R. Pirone, G. Russo, A. Albuquerque, H.O. Pastore, M. Cadoni, A. Frache, L. Marchese, Catal. Commun. 5 (2004) 191.
[86] B.I. Palella, M. Cadoni, A. Frache, H.O. Pastore, R. Pirone, G. Russo, S. Coluccia, L. Marchese, J. Catal. 217 (2003) 100.
[87] M. Kögel, V.H. Sandoval, W. Schwieger, A. Tissler, T. Turek, Chem. Eng. Tech. 21 (1998) 655.
[88] A. Sierraalta, A. Bermudez, M. Rosa-Brussin, J. Mol. Catal. A 228 (2005) 203.
[89] J.A.Z. Pieterse, G.D. Pirngruber, J.A. van Bokhoven, S. Booneveld, Appl. Catal. B 71 (2007) 16.
[90] L. Capek, J. Dedecek, B. Wichterlova, J. Catal. 227 (2004) 352.
[91] J.A. van Bokhoven, D.C. Koningsberger, P. Kunkeler, H. van Bekkum, A.P.M. Kentgens, J. Am. Chem. Soc. 122 (2000) 12842.
[92] A.P. Walker, Catal. Today 26 (1995) 107.
[93] R.J. Blint, J. Phys. Chem. 100 (1996) 19518.